Mutations in *ACTN4*, encoding α-actinin-4, cause familial focal segmental glomerulosclerosis

Joshua M. Kaplan[1]*, Sung Han Kim[1]*, Kathryn N. North[4], Helmut Rennke[3], Lori Ann Correia[1], Hui-Qi Tong[4], Beverly J. Mathis[5], José-Carlos Rodríguez-Pérez[6], Philip G. Allen[2], Alan H. Beggs[4] & Martin R. Pollak[1]

*These authors contributed equally to this work.

Focal and segmental glomerulosclerosis[1] (FSGS) is a common, non-specific renal lesion. Although it is often secondary to other disorders, including HIV infection, obesity, hypertension and diabetes, FSGS also appears as an isolated, idiopathic condition. FSGS is characterized by increased urinary protein excretion and decreasing kidney function. Often, renal insufficiency in affected patients progresses to end-stage renal failure, a highly morbid state requiring either dialysis therapy or kidney transplantation. Here we present evidence implicating mutations in the gene encoding α-actinin-4 (*ACTN4*; ref. 2), an actin-filament crosslinking protein, as the cause of disease in three families with an autosomal dominant form of FSGS. *In vitro*, mutant α-actinin-4 binds filamentous actin (F-actin) more strongly than does wild-type α-actinin-4. Regulation of the actin cytoskeleton of glomerular podocytes may be altered in this group of patients. Our results have implications for understanding the role of the cytoskeleton in the pathophysiology of kidney disease and may lead to a better understanding of the genetic basis of susceptibility to kidney damage.

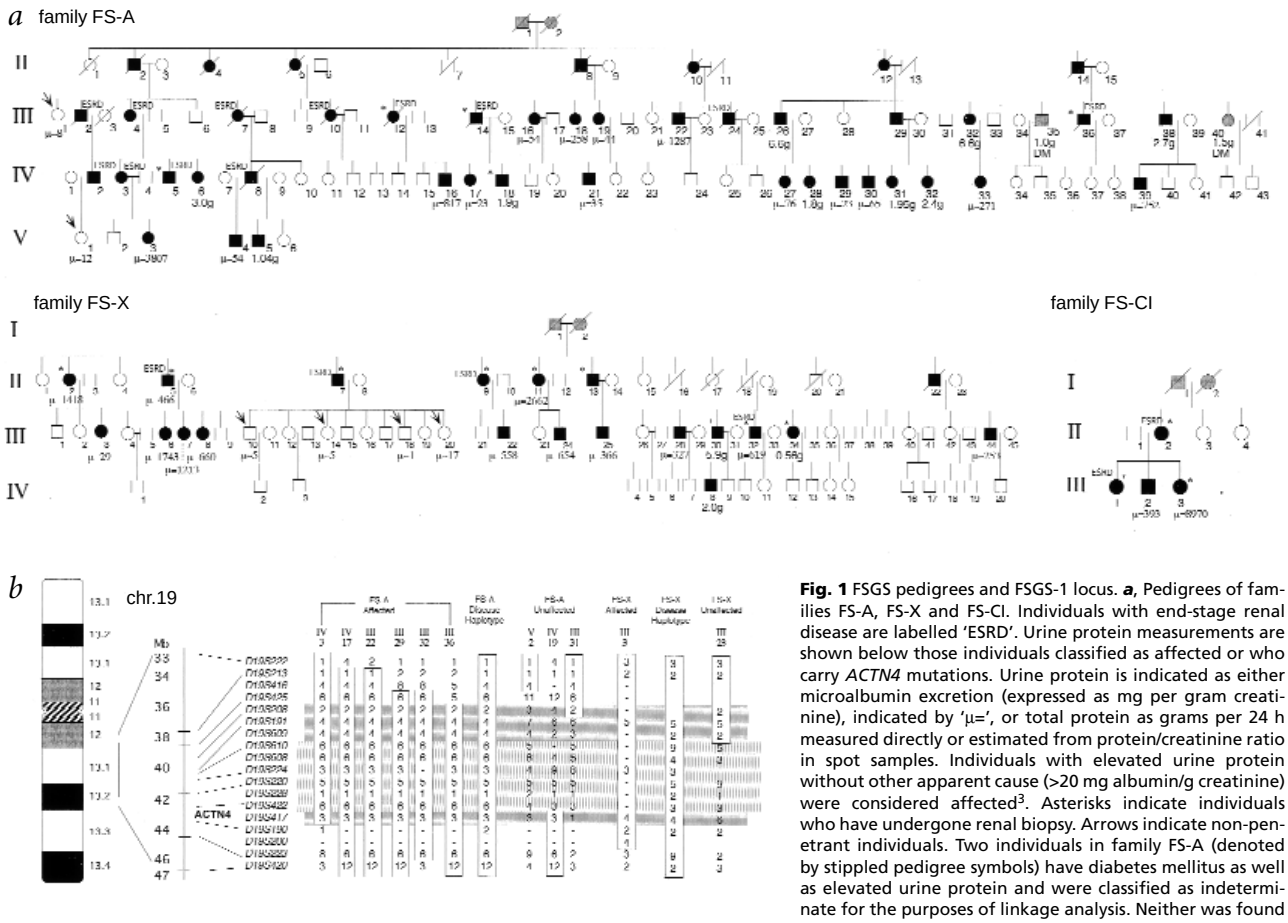

Fig. 1 FSGS pedigrees and FSGS-1 locus. ***a***, Pedigrees of families FS-A, FS-X and FS-CI. Individuals with end-stage renal disease are labelled 'ESRD'. Urine protein measurements are shown below those individuals classified as affected or who carry *ACTN4* mutations. Urine protein is indicated as either microalbumin excretion (expressed as mg per gram creatinine), indicated by 'μ=', or total protein as grams per 24 h measured directly or estimated from protein/creatinine ratio in spot samples. Individuals with elevated urine protein without other apparent cause (>20 mg albumin/g creatinine) were considered affected[3]. Asterisks indicate individuals who have undergone renal biopsy. Arrows indicate non-penetrant individuals. Two individuals in family FS-A (denoted by stippled pedigree symbols) have diabetes mellitus as well as elevated urine protein and were classified as indeterminate for the purposes of linkage analysis. Neither was found to carry the *ACTN4* mutation. Except the two diabetic individuals, every individual with elevated urine microalbumin in each family has inherited the *ACTN4* mutation. ***b***, Illustration of a portion of chromosome 19q showing recombination events which define the FSGS-1 region. For comparison, the disease-associated haplotype seen in the earliest available generation in the two large families is also shown. Recombination events in affected family members restrict the FSGS-1 region to the interval flanked by *D19S425* and *D19S190* when only recombination events in affected individuals are considered (larger, darker rectangle). When recombination events in both affected and unaffected individuals are considered, the minimal genetic interval is restricted to an ~3.5-Mb region (smaller rectangle). *ACTN4* is located between *D19S422* and *D19S417*, which are located ~300 kb apart.

[1]*Renal and* [2]*Hematology Divisions, Department of Medicine, and* [3]*Department of Pathology, Brigham and Women's Hospital, Harvard Medical School, Boston, Massachusetts, USA.* [4]*Genetics Division, Children's Hospital, Harvard Medical School, Boston, Massachusetts, USA.* [5]*Department of Medicine, Oklahoma State University College of Osteopathic Medicine, Tulsa, Oklahoma, USA.* [6]*Nephrology Service, Hospital Ntra Sra del Pino, Las Palmas de Gran Canaria, Spain. Correspondence should be addressed to M.R.P. (e-mail: mpollak@rics.bwh.harvard.edu).*

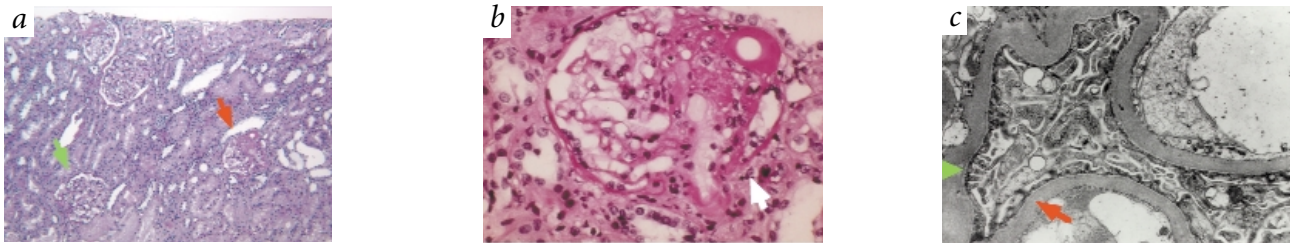

Fig. 2 Kidney biopsies. *a–c*, Renal biopsy from an affected member of family FS-A (light microscopy, PAS stained and electron microscopy). ***a***, A low-power view of several glomeruli, including a relatively normal glomerulus (green arrow) and a diseased glomerulus (red arrow). ***b***, The diseased glomerulus (open arrow), shown at a higher magnifiication, where the arrow indicates the sclerosed half of the glomerulus. In the electron micrograph ***c***), the basement membrane appears to be well preserved. There are regions of preservation of distinct podocyte foot processes (green arrow) as well as regions of glomerular podocyte foot process effacement (red arrow). There is no evidence of a primary basement membrane defect or of immune complex deposition.

FSGS is defined by the presence of segmental sclerosis in some, but not all, glomeruli, and is seen in all ethnic groups, although it is particularly common in individuals of African descent. FSGS may occur as a primary process that is thought to result at least in some instances from a defect in glomerular podocyte function[1]. FSGS may also be inherited as a mendelian trait. Previously, we mapped a gene for autosomal dominant FSGS to human chromosome 19q13 (locus FSGS-1, MIM 603278) in a large family from Oklahoma (FS-A, maximum two-point lod score 12.28 at *D19S191* assuming 95% penetrance; Figs 1 and 2; ref. 3). We subsequently identified a second large family from the Canary Islands (FS-X) with disease mapping to this same locus (lod score 4.44 at *D19S191*; Fig. 1). By genotyping family members at markers on chromosome 19q13, we narrowed the candidate interval to a 3.5-Mb region flanked by *D19S609* and *D19S417* (Fig. 1). In one additional small family from California (FS-CI, Fig. 1), the disease segregated with chromosome 19q13.1 marker alleles. None of the other families we have genotyped show evidence of linkage to 19q13 and the seven largest of these families have excluded it. A second locus for dominant FSGS has been identified on chromosome 11q22–24 in one family[4] and a recessive locus has been reported on chromosome 1q (ref. 5).

Disease in families FS-A, FS-X and FS-CI is similar, with a mild increase in urine protein excretion starting in the teenage years or later, slowly progressive renal dysfunction and the development of end-stage renal failure in some affected individuals. Disease is highly but not fully penetrant. In family FS-A, two individuals carrying the allele associated with the disease have no clinical symptoms. Similarly in family FS-X, four individuals carrying the disease-associated allele have no proteinuria.

We analysed *NPHS1* (encoding nephrin; ref. 6), a candidate on the basis of its genetic localization and involvement in congenital nephrotic syndrome, but failed to find evidence of disease-causing defects. We thus considered other candidate genes. *ACTN4* (ref. 2) was among the genes we found to map to the FSGS-1 region by BLAST comparison of genomic sequence from chromosome 19q13 with GenBank sequence databases. We performed mutational analysis of *ACTN4* because α-actinin is highly expressed in the glomerular podocyte, it is important in non-muscle cytoskeletal function and it is upregulated early in the course of some animal models of nephrotic syndrome[7–10].

We sequenced the entire coding region of reverse-transcribed *ACTN4* from lymphocytes of several affected members of families FS-A and FS-X. We identified heterozygous sequence alterations predicting non-conservative amino-acid substitutions in affected members of both pedigrees (Fig. 3*a*). The A682G and C695T

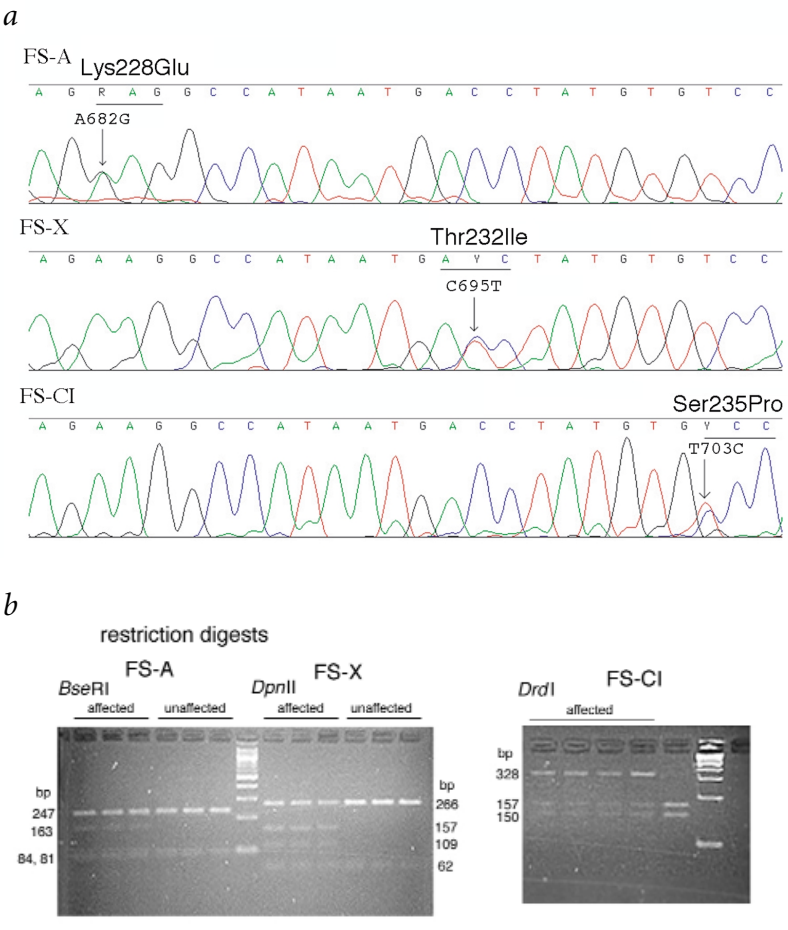

Fig. 3 Mutational analysis. ***a***, Sequence alterations in members of families FS-A, FS-X and FS-CI. Sequencing in families FS-A and FS-X was obtained from PCR-amplifiied reverse transcribed lymphocyte RNA; sequence in family FS-CI was obtained from amplifiied enomic DNA. Heterozygous nucleotide changes are observed, predicting the amino acid changes lysine to glutamate, threonine to isoleucine and serine to proline. ***b***, These changes were predicted to produce new restriction sites for *Bse*RI and *Dpn*II, and loss of a *Drd*I site, respectively. Digestion of PCR-amplifiie *ACTN4* exon 8 confiirmed the presence of these sequenc alterations in affected family members and demonstrated their absence in the control population tested.

human ACTN4	202	EVAEKYLDIPKMLDAEDIVNTARPDE**K**AIM**T**YV**S**SFYHAFSGAQKAETAANRICKVL
family FS-A		----------**E**----------
family FS-X		----------**I**----------
family FS-CI		----------**P**----------
human ACTN1	210	DVAEKYLDIPKMLDAEDIVGTARPDE**K**AIM**T**YV**S**SFYHAFSGAQKAETAANRICKVL
human ACTN2	217	EIAEKHLDIPKMLDAEDIVNTPKPDE**R**AIM**T**YV**S**CFYHAFAGAEQAETAANRICKVL
human ACTN3	224	EVAEKYLDIPKMLDAEDIVNTPKPDE**K**AIM**T**YV**S**CFYHAFAGAEQAETAANRICKVL
rat	210	DVAERYLDIPKMLDAEDIVGTARPDE**K**AIM**T**YV**S**SFYHAFSGAQKAETAANRICKVL
mouse	223	EVAEKYLDIPKMLDAEDIVNTPKPDE**K**AIM**T**YV**S**CFYHAFAGAEQAETAANRICKVL
chicken	222	EVAEKYLDIPKMLDAEDIVNTARPDE**K**AIM**T**YV**S**SFYHAFSGAQKAETAANRICKVL
rabbit	223	EVAEKYLDIPKMLDAEDIVNTPKPDE**K**AIM**T**YV**S**CFYHAFAGAEQAETAANRICKVL
Drosophila	213	DVAEKYLDIPRMLDPDDLINTPKPDE**R**AIM**T**YV**S**CYYHAFQGAQQAETAANRICKVL
Dictyostelium	112	DIAEKELDIPKMLDVSDMLDVVRPDE**R**SVM**T**YV**A**QYYHHFSASRKAETAGKQVGKVL
Trichomonas	201	FAACKELGIYVYLDPEDVIDTT-PDE**K**SVV**T**QV**A**EFFHFFASESKIAAMADKIKRTV
C. elegans	216	DIAEKHLDIPKMLDAEDMANS-QPDE**K**AVM**T**YV**S**CYYHYFSGMRKAETAANRICRVL
β-spectrin (human)	240	NVAERQLGIIPLLDPEDVF-TENPDE**K**SII**T**YV**V**AFYHYFSKMKVLAVEGKRVGKVI

Fig. 4 α-Actinin sequence alignment. Alignment of α-actinin protein sequences including all four human proteins, α-actinins from the other species with available sequence information and human β-spectrin. The amino acid changes seen in each of the three families is indicated. The observed mutations occur in a highly conserved region of the protein.

nucleotide changes cause a lysine-to-glutamate substitution at residue 228 and a threonine-to-isoleucine substitution at residue 232 in families FS-A and FS-X, respectively. Restriction endonuclease digestion confirmed the presence of the mutations in all affected members of each family (as well as those few non-penetrant individuals in each family we previously found to carry the disease-associated allele), as both mutations produce new restriction endonuclease sites (Fig. 3*b*). These mutations were not present in the many unaffected family members or in the (unrelated) spouses, indicating that these sequence changes are not common variants in the local populations. We performed the same assay in a geographically diverse set of individuals (including ethnically appropriate controls) and confirmed that these sequence changes were absent from all 214 alleles. Because the mutations in these families were in close proximity, affecting the region between the actin-binding domain and the first rod domain of the protein[11], we amplified and sequenced the exon encoding this sequence (exon 8) from genomic DNA of members of family FS-CI and found a third distinct missense mutation, T703C, causing a serine-to-proline substitution at residue 235 in all four affected family members. This mutation predicted the loss of a *Drd*I site, which again allowed confirmation of the sequence findings (Fig. 3). This nucleotide change was absent in all 214 control alleles tested. Examination of the remainder of *ACTN4* in an affected member of FS-CI (by RT–PCR and sequencing) showed no evidence of other mutations. All three amino acid residues found to be altered are highly conserved among the four human α-actinin genes, as well as α-actinin genes of all other species (Fig. 4). No other amino acid changes were observed in PCR-amplified exon 8 in 40 normal alleles sequenced.

The α-actinins are actin-binding and crosslinking proteins. There are four known human α-actinin genes, which are highly homologous and highly conserved among species. Expression of *ACTN2* and *ACTN3* is limited to the skeletal and cardiac muscle sarcomere, whereas expression of *ACTN1* and *ACTN4* is widespread[2,12]. In the renal glomerulus, α-actinin has been shown to be localized to podocytes, predominantly in the foot processes, with minimal expression elsewhere[7,8,10]. We performed western-

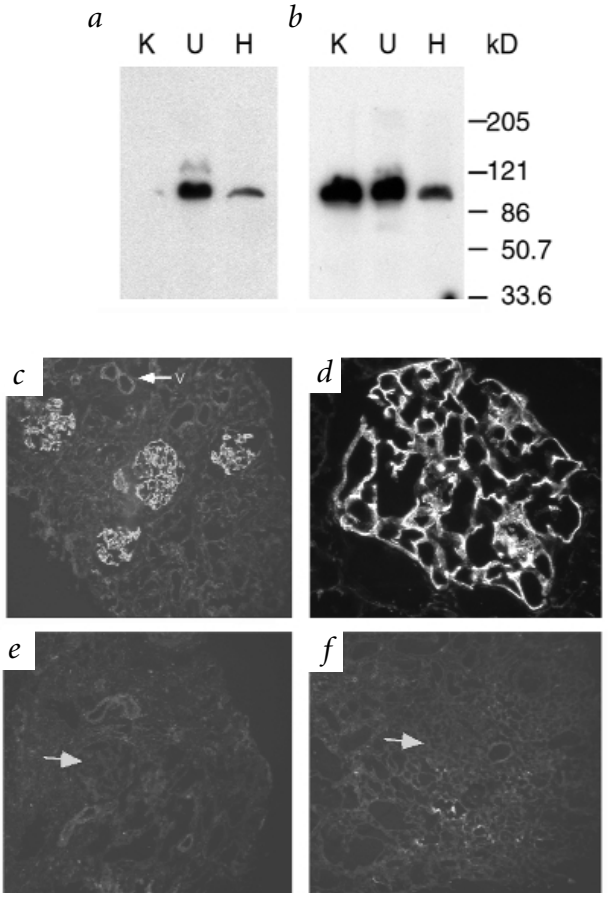

Fig. 5 Analysis of α-actinin-4 expression. ***a***,***b***, Western-blot analysis of whole human tissue lysates from kidney (K), uterus (U) and heart (H) stained with affiinity-purifiied antα–actinin-1 (***a***) or anti-α–actinin-4 (***b***) antibodies. Locations of size markers are indicated at right. Both isoforms are evident as ~100 kD bands. Uterus and heart contain both α-actinin-1 and -4, whereas kidney only contains detectable α-actinin-4. ***c***,***d***, Indirect immunoflluorescence analysi of α-actinin-4 in human kidney (magnifiication×10 and ×40, respectively). There is intense staining of the glomeruli in an epithelial cell pattern. There is also staining of blood vessels (indicated by the arrow and 'V' in *c*). ***e***, Immunoflluorescence staining of the glomruli using anti-α–actinin-1 antisera is minimal. ***f***, Staining with α-actinin-4 pre-immune rabbit serum (×10 magnifiication is also minimal. In the α-actinin-1 and pre-immune serum panels (*e*,*f*), arrows indicate the location of glomeruli.

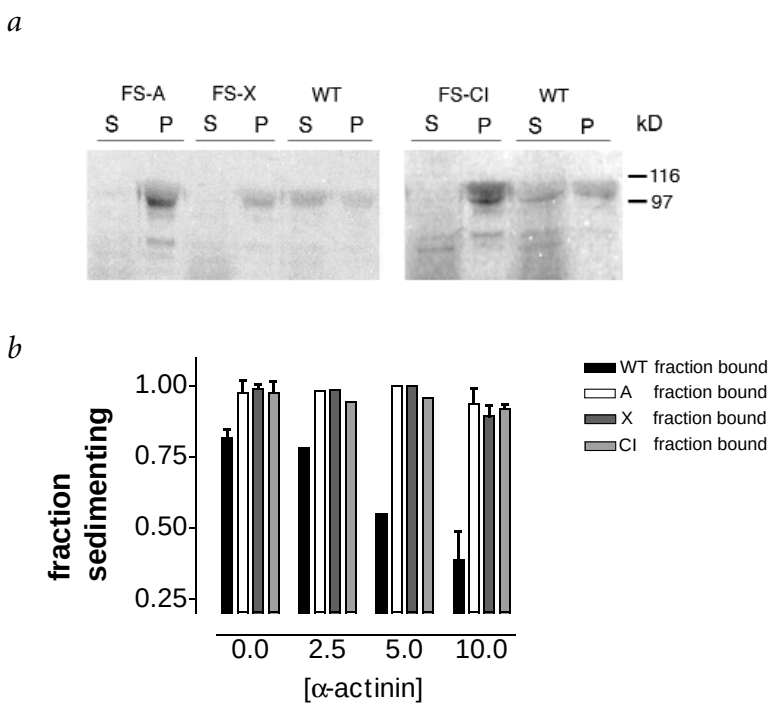

Fig. 6 Actin-binding experiments. ***a***, Gel showing results of actin cosedimentation assays. Supernatant and resuspended pellet were loaded on the gel for each reaction (wild type and each of three mutants). The reactions shown were performed with actin in the presence of cold muscle α-actinin and *in vitro* translated mutant or wild-type α-actinin. Reactions with each of the three mutants and the wild-type α-actinins are shown. S, supernatant; P, pellet. In contrast to wild-type protein, mutant protein was not visible in the supernatants in repeated experiments. ***b***, Graphical representation of the results of cosedimentation experiments conducted in the presence of actin and different amounts of cold α-actinin. Although cold α-actinin competes with the labelled wild-type α-actinin in this assay, essentially all of the mutant α-actinin remains in the pellet even in the presence of 10 μM unlabelled α-actinin, with the amount found in the supernatant not meaningfully distinguishable from background. Three sets of measurements were made with wild type and the three mutants with 0 and 10 μM unlabelled α-actinin present; these results are shown as means with error bars indicating standard deviation. (Other data points shown in the fiigure represent sigle values.) The differences in sedimentation between labelled wild-type actinin and each of the mutants with both 0 and 10 μM cold actinin present was statistically signifiican (two-tailed *P* value ≤0.02 for all mutant/wild-type comparisons using a paired *t* test).

blot and immunofluorescence studies of human kidney using antibodies specific for α-actinin-4 and -1. Western-blot analysis showed no expression of α-actinin-1 in kidney, but did show expression of α-actinin-4 (Fig. 5). We performed immunofluorescence studies to refine the localization of α-actinin-4 within the kidney. We found glomerular staining as well as staining of blood vessels. By contrast, α-actinin-1 and preimmune serum staining of the glomeruli were negative, consistent with the western-blot data (Fig. 5).

To determine whether the identified mutations alter α-actinin function, we introduced these point mutations into the full-length *ACTN4* cDNA and tested the effect on the binding of α-actinin to F-actin[13]. Radiolabelled wild-type and mutant α-actinin-4 translated *in vitro* were incubated with actin under polymerizing conditions. A greater percentage of the mutant actinin cosedimented with F-actin under high-speed centrifugation compared with wild-type α-actinin-4 (Fig. 6). Similar results were observed when actin was allowed to polymerize before the addition of α-actinin. When these experiments were repeated in the presence of increasing competing amounts of unlabelled muscle α-actinin, the sedimentation of labelled wild-type actinin with actin was reduced, as would be expected of the purified protein. By contrast, the cosedimentation of the mutant protein with actin was unchanged, with essentially all of the labelled α-actinin still found in the pellet (Fig. 6). In the absence of actin, no detectable mutant or wild-type labelled α-actinin sedimented under 100,000*g* centrifugation, indicating that the mutant protein was not aggregating. A control plasmid (luciferase) translated *in vitro* did not cosediment with actin filaments. These observations are consistent with the hypothesis that these FSGS-associated mutations increase the binding of α-actinin to actin filaments.

On the basis of the genetic, expression and functional evidence, we conclude that mutations in *ACTN4* cause or increase susceptibility to focal segmental glomerulosclerosis. Future studies will more clearly define the role of α-actinin-4 and these specific α-actinin alterations in glomerular function. The effect of these mutations on kidney function and structure may be the most readily apparent phenotype because of the high level of expression of α-actinin-4 in the podocyte[10,14] and the unique architecture of the glomerulus. These dominant mutations may alter the interaction of α-actinin with actin filaments *in vivo*, altering the mechanical characteristics of the glomerular podocyte by interfering with normal filament assembly and disassembly. In addition to actin, there are a number of other proteins that interact with α-actinin[15–21], and it may be that an alteration in one or more of these interactions is critical to disease pathogenesis. Other models are also possible. As α-actinin-4 is also expressed in capillaries as well as larger blood vessels[2], a change in the renal vascular cytoskeleton might alter glomerular haemodynamics and contribute to the observed phenotype.

Previous reports have shown that humans with altered nephrin and mice homozygous for targeted deletions of *Cd2ap* display severe early onset nephrosis, providing insight into the molecular pathogenesis of proteinuria[6,22]. Nephrin is a major component of the glomerular slit diaphragm[23]; Cd2ap interacts with nephrin and may serve to anchor it to the cytoskeleton. Our finding that mutations in *ACTN4* cause FSGS indicates that the actin cytoskeleton itself may be involved in the pathogenesis of proteinuria, perhaps through an effect on the slit diaphragm structure. Further, given the genetic heterogeneity of familial FSGS, it is reasonable to speculate that other components of the actin cytoskeleton may be disrupted in other families with FSGS. A final possibility is that alterations in the actin cytoskeleton may represent a proximal component of the renal response to primary insults causing secondary glomerular disease, and thus the actin cytoskeleton may represent a target for therapeutic intervention for prevention of glomerulosclerosis.

Methods

Clinical material. Blood was obtained from family members after informed consent was given in accordance with a protocol approved by the Institutional Review Board at the Brigham and Women's Hospital. Descriptions of families FS-A and FS-X have been reported[3,24,25]. We considered family members to be affected if they fulfilled the following criteria[3]: (i) renal failure or renal insufficiency in the absence of other

cause; (ii) any increase in urine microalbumin excretion above normal in the absence of another apparent cause; or (iii) focal segmental glomerulosclerosis apparent on renal biopsy. Patients with long-standing diabetes mellitus and proteinuria were considered indeterminate. We derived EBV-transformed lymphoblastoid cell lines from members of families FS-A and FS-X by standard methodology[26]. Genomic DNA extraction from blood was performed using Qiagen columns. Measurement of urine microalbumin was performed by Quest Diagnostics.

Genotyping. We genotyped DNA samples at markers on chromosome 19q by PCR amplification of genomic DNA using one γ^{P-32}-dATP end-labelled primer, electrophoresis on a 6% polyacrylamide gel and exposure to radiographic film. We purchased marker primers (Research Genetics and Integrated DNA Technologies).

Sequence analysis. We accessed chromosome 19q sequence through the Lawrence Livermore National Laboratory Genome Center web site (http://www-bio.llnl.gov/bbrp/genome/). We accessed the BLAST program through the National Center for Biotechnology Information web site (http://www.ncbi.nlm.nih.gov/), which we used for comparison of genomic sequence to the EST and non-redundant GenBank databases.

Amplification and sequencing of *ACTN4*. We isolated RNA from transformed lymphocytes (FS-A and FS-X) or blood (FS-CI) using Trizol reagent. We performed reverse transcription using a Superscript kit (GIBCO/BRL) with oligo-dT and random hexamers for priming. We designed primer pairs to amplify the *ACTN4* coding sequence. We performed PCR amplification in 25 µl reactions (using primer pairs 3′UTR-R, 5′–GGAG GACTGCAGAGAGTGCTTTGC–3′, and 2135F, 5′–CAGCACCAGCTCAT CCAGGAGGC–3′; 1054F, 5′–GAAGTGCCAGCTGGAGATCAACTTC–3′, and 2190R, 5′–GTATAGTTGGTGTGCTTGTTGTCG–3′; –66F, 5′–CGC GGCGAACCAGTCGTACCAG–3′, and 1105R, 5′–GAGGCGCAGCTTG GTCTGCAGC–3′. We purified amplicons by electrophoresis on an agarose gel and extraction from the gel slices using a Qiaex II kit. We sequenced these products in affected members of families FS-A, FS-X and FS-CI using these forward and reverse primers as well as primers 1598F (5′–CTG GAATACGCCAAGCGCGCGGC–3′), 1645R (5′–GCTCTCCATCCAGTT GTTGAAGG–3′), 518F (5′–CTCTGGTGCCAGAGAAAGACAGC–3′) and 565R (5′–CTGCACATTGACGTTCTTATACG–3′) using an ABI377 automated sequencer at the core facilities at the Brigham and Women's Hospital. Mutations A682G and C695T predicted the creation of novel restriction sites and mutation T703C predicted the loss of a restriction site. We used PCR-amplified genomic DNA to confirm the presence of mutations in the other family members and to examine controls. We designed primers for amplification of *ACTN4* exon 8 by comparison of cDNA sequence with genomic sequence at the Lawrence Livermore National Laboratory Genome Center web site (8F, 5′–CCCAAGTCACGCGTCACTCT GC–3′, 8R, 5′–GAGAGAGGCCACTGCCGTCTGC–3′). We sequenced PCR-amplified exon 8 DNA as above. We performed restriction digests using *Dpn*II, *Bse*RI and *Drd*I to detect the presence or absence of heterozygosity for the nucleotide change in 40 µl reactions following the manufacturer's instructions (New England Biolabs).

Immunofluorescence. We generated rabbit polyclonal antisera specific for α-actinin-1 and -4 using isoform-specific polypeptides derived from unique amino-terminal sequences DHYDSQQTNDYMQPC (α-actinin-1) and NQSYQYGPSSAGNGAGC (α-actinin-4), which were conjugated to keyhole limpet haemocyanin via the added carboxy-terminal cysteines. We immunized two rabbits with each peptide and each pair generated antibodies with similar properties. Neither peptide bears any resemblance to sequences in other known α-actinin isoforms and each antiserum reacted with the expected ~100-kD protein in a unique tissue-specific pattern consistent with lack of cross-reactivity between the isoforms. We performed western-blot analysis and indirect immunofluorescence as described[27,28]. Immunofluorescence experiments using crude antisera at dilutions of 1:200 to 1:1,000 gave similar results to those using affinity-purified preparations. We incubated ethanol-fixed sections with primary rabbit anti-α–actinin-4 and -1 antisera, preimmune serum and secondary Cy3-labelled antibodies all diluted 1:200 in PBS. We captured immunofluorescence images using a Princeton Instruments MicroMax 5 Mz 1300 by 1030 Interline cooled CCD camera (Roper Instruments) and Esee software (Inovision). We imaged each sample for the same 0.2-s time period.

Actin-binding experiments. We made expression constructs for *in vitro* transcription of *ACTN4* using the insert from a full-length human *ACTN4* cDNA originally cloned by degenerate PCR as described[12]. We inserted the A682G (family FS-A) and C695T (family FS-X) mutations into a full-length *ACTN4* cDNA in pBluescript SK II by replacement of a *Bst*XI/*Bam*HI fragment in the cDNA (nt 639–842) with the equivalent fragment obtained by RT–PCR amplification from transformed FS-A and FS-X affected family member lymphocytes and endonuclease digestion. We sequenced the *ACTN4* clones, confirming that they differed from the wild type only by the desired single-nucleotide substitutions. We inserted the T703C mutation (family FS-CI) into the cDNA using the QuickChange kit (Stratagene) with forward and reverse 25-mers incorporating the mutant nucleotide following the manufacturer's directions. The sequence of the wild-type *ACTN4* clone used in these studies matched the previously reported cDNA sequence[2].

We perfomed *in vitro* translation of mutant and wild-type *ACTN4* using a TnT Coupled Reticulocyte Lysate kit (Promega) in the presence of S-35-methionine and plasmid DNA (500 ng). Electrophoresis on a 7.5% acrylamide gel and exposure of the dried gel to radiographic film confirmed the presence of the expected ~100 kD product from each reaction. We incubated labelled *in vitro* translated product (5 µl) from a 50 µl reaction in an 80 µl reaction containing KCl (100 mM), $MgCl_2$ (2 mM), ATP (0.5 mM), 0.2 mM DTT, Tris (10 mM, pH 7.4; conditions in which non-specific protein binding to actin is minimized), G-actin (6 µM) and varying concentrations of purified cold rabbit skeletal muscle α-actinin (both obtained from Cytoskeleton). We allowed actin to polymerize in this buffer for 60 min at RT. We also performed reactions in which actin was allowed to polymerize before the addition of α-actinin and obtained similar results. We centrifuged the reactions at 100,000*g* for 30 min at 18 °C. We removed the supernatants for gel analysis and resuspended the pellet in the initial 80 µl volume. We performed electrophoresis using each resuspended pellet (20 µl) and supernatant and a 7.5% polyacrylamide gel, which we dried and exposed to radiographic film. We quantitated the intensity of the 100-kD bands using PhosphoImager (Molecular Dynamics) software and expressed the amount of α-actinin which sedimented as a percentage of the total detected in the pellet plus the supernatant.

GenBank accession numbers. *ACTN4*, U48734, D89980; *ACTN1*, X15804; *ACTN2*, NP_001094; *ACTN3*, M86407; *SPTB*, J05500. Actinin from other species: rat, AAD12064; mouse, AF093775; chicken, Q90734; rabbit S17548; *Drosophila melanogaster*, AL031765; *Dictyostelium*, g929034; *Trichomonas*, AF014928; *Caenorhabditis elegans*, CAA99944.

Acknowledgements

We thank the family members for participation; members of the Department of Genetics, Harvard Medical School and the Department of Medicine at Brigham and Women's Hospital, particularly B. Denker, for helpful discussions; A. Shahsafaei for help with immunofluorescence; L. Ashworth for help with chromosome 19 sequence informatics; M. Dolliver for help with clinical ascertainment; and members of the core sequencing facilities and the Genome Center at the Brigham and Women's Hospital for their assistance. This work was supported by NIH grants DK54931 (M.R.P.), AR44345 and AR02026 (A.H.B.), GM57256 (P.G.A.) and a National Research Service Award (J.M.K.), as well as grants from the National Kidney Foundation and the Burroughs Wellcome Fund (M.R.P.) and the Muscular Dystrophy Association (A.H.B.).

Received 12 October 1999; accepted 14 January 2000.

1. Ichikawa, I. & Fogo, A. Focal segmental glomerulsoclerosis. *Pediatr. Nephrol.* **10**, 374–391 (1996).
2. Honda, K. *et al.* Actinin-4, a novel actin-bundling protein associated with cell motility and cancer invasion. *J. Cell. Biol.* **140**, 1383–1393 (1998); erratum: **143**, 276 (1998).
3. Mathis, B.J. *et al.* A locus for inherited focal segmental glomerulosclerosis maps to chromosome 19q13: Rapid Communication. *Kidney Int.* **53**, 282–286 (1998).
4. Winn, M. *et al.* Linkage of a gene causing familial focal segmental glomerulosclerosis to chromosome 11 and further evidence of genetic heterogeneity. *Genomics* **58**, 113–120 (1999).
5. Fuchshuber, A. *et al.* Mapping a gene (SRN1) to chromosome 1q25–q31 in idiopathic nephrotic syndrome confirms a distinct entity of autosomal recessive nephrosis. *Hum. Mol. Genet.* **4**, 2155–2158 (1995).
6. Kestila, M. *et al.* Positionally cloned gene for a novel glomerular protein—nephrin—is mutated in congenital nephrotic syndrome. *Mol. Cell* **1**, 575–582 (1998).
7. Drenckhahn, D. & Franke, R.P. Ultrastructural organization of contractile and cytoskeletal proteins in glomerular podocytes of chicken, rat, and man. *Lab. Invest.* **59**, 673–682 (1988).
8. Smoyer, W.E., Mundel, P., Gupta, A. & Welsh, M.J. Podocyte α-actinin induction precedes foot process effacement in experimental nephrotic syndrome. *Am. J. Physiol.* **273**, F150–157 (1997).
9. Shirato, I., Sakai, T., Kimura, K., Tomino, Y. & Kriz, W. Cytoskeletal changes in podocytes associated with foot process effacement in Masugi nephritis. *Am. J. Pathol.* **148**, 1283–1296 (1996).
10. Kurihara, H., Anderson, J.M. & Farquhar, M.G. Increased Tyr phosphorylation of ZO-1 during modification of tight junctions between glomerular foot processes. *Am. J. Physiol.* **268**, F514–524 (1995).
11. Djinovic-Carugo, K., Young, P., Gautel, M. & Saraste, M. Structure of the α-actinin rod: molecular basis for cross-linking of actin filaments. *Cell* **98**, 537–546 (1999).
12. Beggs, A.H. *et al.* Cloning and characterization of two human skeletal muscle α-actinin genes located on chromosomes 1 and 11. *J. Biol. Chem.* **267**, 9281–9288 (1992).
13. Wachsstock, D.H., Schwartz, W.H. & Pollard, T.D. Affinity of α-actinin for actin determines the structure and mechanical properties of actin filament gels. *Biophys. J.* **65**, 205–214 (1993).
14. Drenckhahn, D., Schnittler, H., Nobiling, R. & Kriz, W. Ultrastructural organization of contractile proteins in rat glomerular mesangial cells. *Am. J. Pathol.* **137**, 1343–1351 (1990).
15. Eilertsen, K.J., Kazmierski, S.T. & Keller, T.C. III Interaction of α-actinin with cellular titin. *Eur. J. Cell. Biol.* **74**, 361–364 (1997).
16. Carpen, O., Pallai, P., Staunton, D.E. & Springer, T.A. Association of intercellular adhesion molecule-1 (ICAM-1) with actin-containing cytoskeleton and α-actinin. *J. Cell Biol.* **118**, 1223–1234 (1992).
17. Papa, I. *et al.* α-actinin-CapZ, an anchoring complex for thin filaments in Z-line. *J. Muscle Res. Cell Motil.* **20**, 187–197 (1999).
18. Fukami, K., Endo, T., Imamura, M. & Takenawa, T. α-Actinin and vinculin are PIP2-binding proteins involved in signaling by tyrosine kinase. *J. Biol. Chem.* **269**, 1518–1522 (1994).
19. Sampath, R., Gallagher, P.J. & Pavalko, F.M. Cytoskeletal interactions with the leukocyte integrin β2 cytoplasmic tail. Activation-dependent regulation of associations with talin and α-actinin. *J. Biol. Chem.* **273**, 33588–33594 (1998).
20. Reinhard, M. *et al.* An α-actinin binding site of zyxin is essential for subcellular zyxin localization and α-actinin recruitment. *J. Biol. Chem.* **274**, 13410–13418 (1999).
21. Pomies, P., Louis, H.A. & Beckerle, M.C. CRP1, a LIM domain protein implicated in muscle differentiation, interacts with α-actinin. *J. Cell Biol.* **139**, 157–168 (1997).
22. Shih, N.Y. *et al.* Congenital nephrotic syndrome in mice lacking CD2-associated protein. *Science* **286**, 312–315 (1999).
23. Holzman, L.B. *et al.* Nephrin localizes to the slit pore of the glomerular epithelial cell. *Kidney Int.* **56**, 1481–1491 (1999).
24. Mathis, B.J., Calabrese, K.E. & Slick, G.L. Familial glomerular disease with asymptomatic proteinuria and nephrotic syndrome: a new clinical entity. *J. Am. Osteopath. Assoc.* **92**, 875–884 (1992).
25. Tomero, J.S. *et al.* Focal segmental glomerulosclerosis in three generations of a single family. *Int. J. Pediatr. Nephrol.* **6**, 199–204 (1985).
26. Ausubel, R.M. *et al. Current Protocols in Molecular Biology* (Greene, New York, 1995).
27. North, K.N. & Beggs, A.H. Deficiency of a skeletal muscle isoform of α-actinin (α-actinin-3) in merosin-positive congenital muscular dystrophy. *Neuromuscul. Disord.* **6**, 229–235 (1996).
28. North, K.N. *et al.* A common nonsense mutation results in α-actinin-3 deficiency in the general population. *Nature Genet.* **21**, 353–354 (1999).